Hindawi
Geofluids
Volume 2022, Article ID 8237954, 16 pages
https://doi.org/10.1155/2022/8237954

Research Article

Study on Deformation Mechanism and Control Measures of Tanziyan Landslide

Hai-chuan Tao,[1] Yuan Zhang,[1] Jia-xing Dong,[2] Zhi-qiang Zhou,[2] Xin-yue Gong,[2] and Sheng-wei Zhang[2]

[1]*Hydrogeology and Engineering Geology Brigade of Hubei Geological Bureau, Jingzhou 434020, China*
[2]*Faculty of Electric Power Engineering, Kunming University of Science and Technology, Kunming, Yunnan 650500, China*

Correspondence should be addressed to Jia-xing Dong; dong1986@kust.edu.cn

Received 10 January 2022; Revised 18 February 2022; Accepted 21 February 2022; Published 29 March 2022

Academic Editor: Long Yan

Copyright © 2022 Hai-chuan Tao et al. This is an open access article distributed under the Creative Commons Attribution License, which permits unrestricted use, distribution, and reproduction in any medium, provided the original work is properly cited.

Studying the deformation and failure mechanism of the Tanziyan landslide in Yesanguan Town, Badong County, and designing the controlling measures are of great significance to ensure the sustainable development of urban planning and construction. In this paper, stability of Tanziyan landslide is analyzed using the calculation method of complex plane slip surface. After consideration of the essential characteristics of the disaster body,the deformation and failure mechanism of the landslide is studied, and the corresponding landslide treatment measures are presented. Results show stability state of the landslide is understable to unstable as a whole, and the development process can be roughly divided into three stages: sliding, bending and the cracks are connected. Finally, it is proposed to cut and reshape the slope from the crack groove on the slope top to the national highway, and thenlattice beams and anchor cables are presented to protect the reshaped slope surface. Ecological bags are used to stack and regreen between the lattice structures. A retaining wall is built on the inner side of the national highway at the bottom of the slope cutting area, an active protective net is laid on the east side of the crack groove, and monitoring works are set for potential deformation areas. In short, experiences of engineering practice in this landslidecan provide reference for similar projects.

1. Introduction

Landslide has always been a major type of geological disaster in mountainous areas. Landslide will lead to local traffic interruption, power facility damage, and villagers' forest land damage, threaten people's life safety, and cause serious economic losses. It is of great significance to find out the geological environmental conditions of landslides, clarify the deformation and failure mechanism, and put forward reasonable and scientific treatment measures for landslide prevention and control. In terms of landslide deformation and failure mechanism, many researchers start with engineering geological conditions, establish geological models, and deeply analyze its stability and deformation and failure mechanism. For example, Yao [1] took the Gedui village landslide in the Nujiang river basin as an example. Based on a geological survey, the whole process from landslide deformation accumulation to failure using discrete element numerical simulation technology was simulated. Liu et al. [2] found out the engineering geological conditions of landslide on the slope during the construction of the Zhuxi expressway. They analyzed the deformation, development, failure characteristics, and genetic mechanism of landslide in combination with geological mapping and survey. Zhang et al. [3] took the instability of sand mudstone-interbedded slope in road engineering as an example and comprehensively considered multiple factors such as slope structure, stratum structure, and microstructure. The deformation and failure mode of multifree surface combination and unequal thickness interbedded rock slope is analyzed. The corresponding treatment measures are put forward according to the deformation and failure mode. Zeng et al. [4] systematically studied the characteristics and deformation instability mechanism of Zhaojiagou landslide in Zhenxiong County based on the basic data obtained from several landslide field investigations and

exploration. Zhang et al. [5] used MIDAS/GTS software to conduct three-dimensional numerical simulation studies on the formation mechanism of the Liujiapo landslide. Xu [6] analyzed and summarized the deformation and failure behavior and deformation time curve of various landslides, combined with the rheological test results of rock and soil mass, and according to the characteristics of slope deformation curve with time changing, the landslides are divided into three types: stable type, gradual change type, and sudden type, and the mechanical conditions for these three types of deformation behavior are given. Hu et al. [7] analyzed the formation mechanism of the Baozha landslide based on the systematic study of the engineering geological conditions of the landslide. In addition, external factors such as dry-wet cycle, freeze-thaw cycle, and natural cracks have a significant impact on the deformation and failure of the slope. Under the influence of long-term rainfall and sunlight, the rock mass in nature will inevitably change its structure and develop cracks, thus affecting the stability of the slope. Li et al. [8, 9] studied sandstone's deformation and failure mechanism from the macro- and microperspectives by observing the microstructure of the specimen before and after failure through different dry-wet cycles of sandstone, followed by uniaxial compression test and direct shear test. Wang et al. [10] proposed a coupled damage model based on digital image processing technology, freeze-thaw cycle, and uniaxial cyclic load test, which can well describe the damage accumulation of rock, and the influence of natural cracks at rock deformation and failure is undeniable pronounced. Gao et al. [11, 12] carried out systematic field monitoring on a coal mine area and determined the evolution process of crack network in coal and rock mass by using fractal geometry and algorithm of predicting connectivity rate. At the same time, based on uniaxial compression test and digital image processing technology, it is pointed out that the tensile deformation of the original fracture can lead to fracture consolidation. Under high loading rate, the main reason for rock mass failure is fracture consolidation. Zhu et al. [13] studied the evolution process of intergranular cracks in granite with temperature from a microperspective. They pointed out that with the increase of temperature, the number of internal cracks increases, resulting in the gradual separation of mineral particles, that is, the internal structure of rock is broken, which affects the stability of slope. According to Chen et al. [14], the performance of the analytical solution is verified by comparing it with the results of numerical tests obtained using the three-dimensional distinct element code (3DEC), leading to a reasonably good agreement. The analytical solution quantitatively demonstrates that the equivalent elastic modulus increases substantially with an increase in confining stress. It is characterized by stress dependency. Zhu et al. [15] conducted 16 uniaxial cyclic loading simulations with distinct loading parameters related to reservoir conditions (loading frequency, amplitude level, and maximum stress level) and different water contents. The numerical results show that all these three loading parameters affect the failure characteristics of sandstone, including irreversible strain, damage evolution, strain behavior, and fatigue life.

In terms of landslide treatment, applicable conditions and applicability of various prevention and control measures should be analyzed in detail. The typical treatment schemes include bypassing the landslide area, weight reduction, back pressure, drainage, and retaining works [16–21] for many landslide treatment projects, which are often applied comprehensively. For example, according to Zhu et al. [22], constant resistance and large deformation bolt have excellent characteristics of high constant resistance force, large deformation, and high energy absorption and are thus widely used in the reinforcement and monitoring of roadway, tunnel, and slope engineering. Zou [23] designed antislide piles to stabilize the slope according to the stability calculation results and carried out landslide prevention and treatment by laying asphalt macadam in the middle and lower part of the landslide, placing gabion net in the middle and upper part of the landslide, and planting with full vegetation coverage. Huang [24], based on the landslide problem of Meihe expressway, analyzed the causes of slope landslide, puts forward the reinforcement scheme for anchor cable frames beam and anchor lattice beam, and puts forward the matters needing attention to drainage design and construction. Cao [25] studied the causes of the giant ancient landslide on the left bank on Xiluodu hydropower station and carried out construction and monitoring by taking engineering measures such as deep and shallow drainage, presser foot slope concrete, frame beam, and anchor cable foot fixation, to ensure the stability of the ancient landslide. Tao et al. [26] conducted the reinforcement mechanism test of layered anti-inclined slope based on physical model and determined the instability failure of anti-inclined slope reinforced with negative Poisson's ratio anchor. Li et al. [27] studied the mechanical behavior of surrounding rocks under prestressed anchor support, and a mechanical model is established. It is determined that the main controlling factors of the support effect are prestressing, anchor cable length, and anchor cable spacing. Similar simulation verification experiments further substantiated the accuracy of numerical simulation. The results indicate that the numerical simulation method of ubiquitous joint and DFN (discrete fracture network) can attain accurate results. Above all, controlling measures of the Tanziyan landslide should be designed after studying the deformation and failure mechanism.

2. Project Description

From June 19 to June 25, 2018, Tanziyan had a significant landslide risk. The accumulation caused by deformation and damage blocked about 100 m of the National Highway 318 (G318), resulting in damage to ancillary road facilities and transmission lines, with a direct economic loss of 6.425 million yuan. According to professional monitoring data, the Tanziyan landslide geological disaster has apparent mountain displacement and poor stability. Under the influence of continuous heavy rainfall, it is very likely to produce large-scale landslide deformation again, which will cause more severe consequences. If the Tanziyan landslide is unstable as a whole, many accumulations roll down at the bottom of the slope, blocking the Yuquan river and forming dammed lakes, and it will pose a significant threat to the downstream residents.

Therefore, once the Tanziyan landslide geological disaster is unstable, the loss is enormous. The potential catastrophe is highly unfavorable to the sustainable development of local economy and urban planning and construction. The comprehensive treatment of the Tanziyan landslide geological disaster is vital and urgent, with practical economic significance and important social significance.

2.1. Geographical Conditions. The study area is in Tanziyan, group 15, Tanjia village, Yesanguan Town, Badong County, Hubei Province (Figure 1), where the steep slope inside the K1420 + 000 − K1420 + 600 section of G318. The geographical coordinates are 30°38′57.5″N and 110°19′55.6″E, and village road and G318 are connected around the landslide site, with convenient transportation.

Tanziyan landslide geological hazard body is located on the hill from south to north, the bottom of the hill is Yuquan river, and the middle of the slope is G318, that is, the front edge of the landslide body. The rear rim is a ridge, the left side is a natural concave slope, and the new bedrock escarpment bounds the right side.

The exploration area is located on the right bank of the Yuquan river, with a peak elevation of 1100~1147 m and a relative elevation difference of 240~287 m. The microgeomorphic combination of the area is canyon steep slope. The sloped body is a clockwise slope composed of thick layer massive chert nodule limestone of Maokou Formation (P_1m) of Lower Permian system. The terrain is generally high in the south and low in the north. The lowest point is the bottom of the Yuquan river valley, with an elevation of 860 m. The valley profile presents an asymmetric "V" shape, and the left bank is a cliff, mainly formed by uncanny craft. The right bank slope is slightly slower than that of the left bank. The profile is linear with a steep bottom and soft folding top. The slope of the lower slope is 45~60°, and the slope of the upper slope is 30~45°. G318 runs parallel to the river valley in the middle of the proper bank slope, with an elevation of 1003-1009 m. The landslide area is located inside G318.

2.2. Geological Environment. According to relevant survey data, the working area belongs to structural erosion dissolution deep cutting medium mountain geomorphology, and the basic terrain configuration is platform mountain and deep valley. The terrain is high in the north and low in the south, the peak elevation is 1593~1100 m, and the cutting depth of the valley is 200~700 m. The southern part of the survey area is a ridge mountain canyon with the disintegration of the plateau, and the height decreases. The mountains are affected by the NE and EW structures of the region. Therefore, they generally extend along with the NE and EW directions.

Yangchang river anticline (Z1), Chenjiaya syncline (Z2), Yesanguan anticline (Z3), and Xiangbanxi syncline (Z4-1, 4-2, and 4-3) are mainly developed in the working area. Secondary small folds can be seen everywhere in the survey area, and joint fissures are relatively developed. The faults mainly include Zigui-Yesanguan fault, Yesanguan fault, general fault, and Yuejiahuang fault. Zigui Yesanguan fault and Yesanguan fault are close to the study area. The rock fissures are relatively developed, which has a significant impact on the integrity of nearby rock strata and slope stability. Other faults are far away from the study area and have a slight effect on the rock stratum in the working area, as shown in Figure 2. In short, fractures are highly developed due to the development of faults, anticlines, and other structures in the area. The fractures in the area are mainly inclined to the north, which is conducive to the development of slope unloading fracture structural plane through cutting layers, especially those whose tendency is consistent with the slope surface and whose inclination angle is close to or less than the slope angle having a significant impact on slope stability.

The lithology of the stratum in the area is single, mainly exposing upper Paleozoic carbonate strata, followed by quaternary eluvial, colluvial diluvial, and artificial accumulation. The surface water in the survey area is poor, mostly the surface flow and runoff formed by atmospheric precipitation quickly, which is discharged and collected down the Yuquan river along the mountain. The karst in the Yuquan river is developed, and the river bed is a dry ditch in arid season, so it is speculated that the groundwater is rich.

2.3. Basic Characteristics of Disaster Bodies. The plane shape of the Tanziyan landslide body is irregular armchair shape, with a longitudinal length of about 146 m, an average width of 250 m, and an area of about $3.65 \times 10^4\ m^2$, the average thickness is about 12.0 m, and the total volume is about $43 \times 10^4\ m^3$, which is a medium-sized geotechnical mixed landslide, with the main sliding direction of about 347°, as shown in Figure 3. At present, there are three small pitches and one collapse. Among them, three slopes are located on the inner side of the front national highway, arranged in a straight line from east to west, with deformation and failure volume of $750\ m^3$, $3500\ m^3$, and $7875\ m^3$, respectively. The collapse body is located near the top of the slope in the west, and the collapse volume is about $2460\ m^3$.

The boundary conditions of the Tanziyan landslide are apparent. The front edge is direct to G318, distributed in the northeast-southwest direction, with free conditions for landslide development. The trailing edge is bounded by the drawing crack trough at the ridge with 235° strike, with an elevation of 1115.7 m. The drawing crack trough is broad in the southwest and narrow in the northeast. The widest part of the tensile fracture groove is 5 m and 19.8 m deep. Its distribution direction is 235°. After pinching to the east, multiple intermittent tensile fractures are developed and distributed in the echelon. The left margin is bounded by a depression set in the southeast direction. The right boundary is determined by the arc cliff extending from northeast to near north.

Tanziyan landslide is divided into two areas according to the current deformation: deformation area and potential deformation area. The deformation area is located on the left side of the Tanziyan landslide. The width of the deformation area is about 120 m. The primary deformation is top collapse, ground crack, and bottom collapse deformation. The potential deformation area is located on the right where no obvious deformation has been found. Still according to the

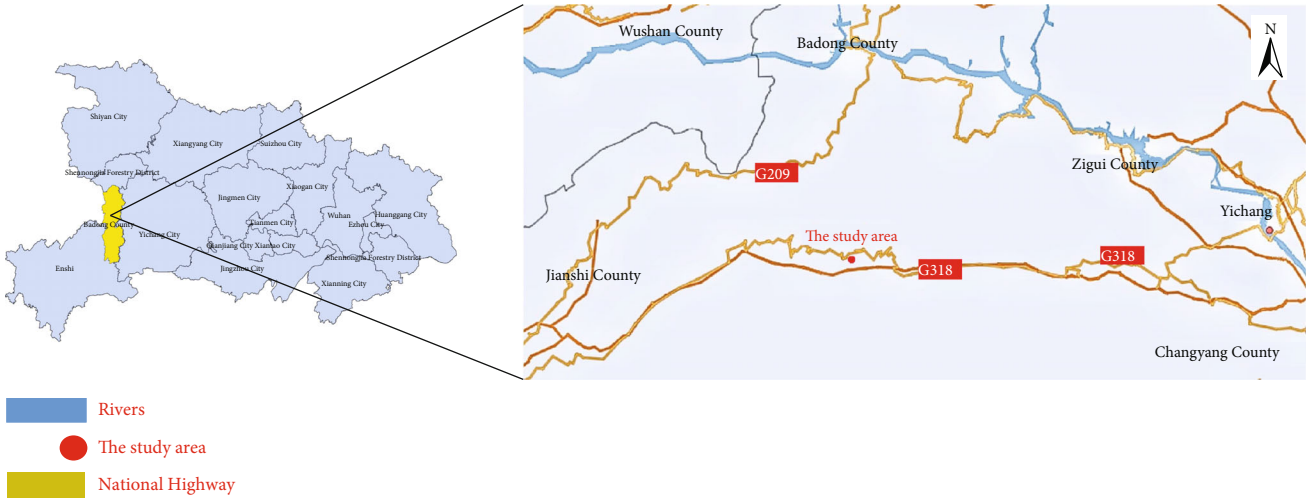

Figure 1: Geographical location of the study area.

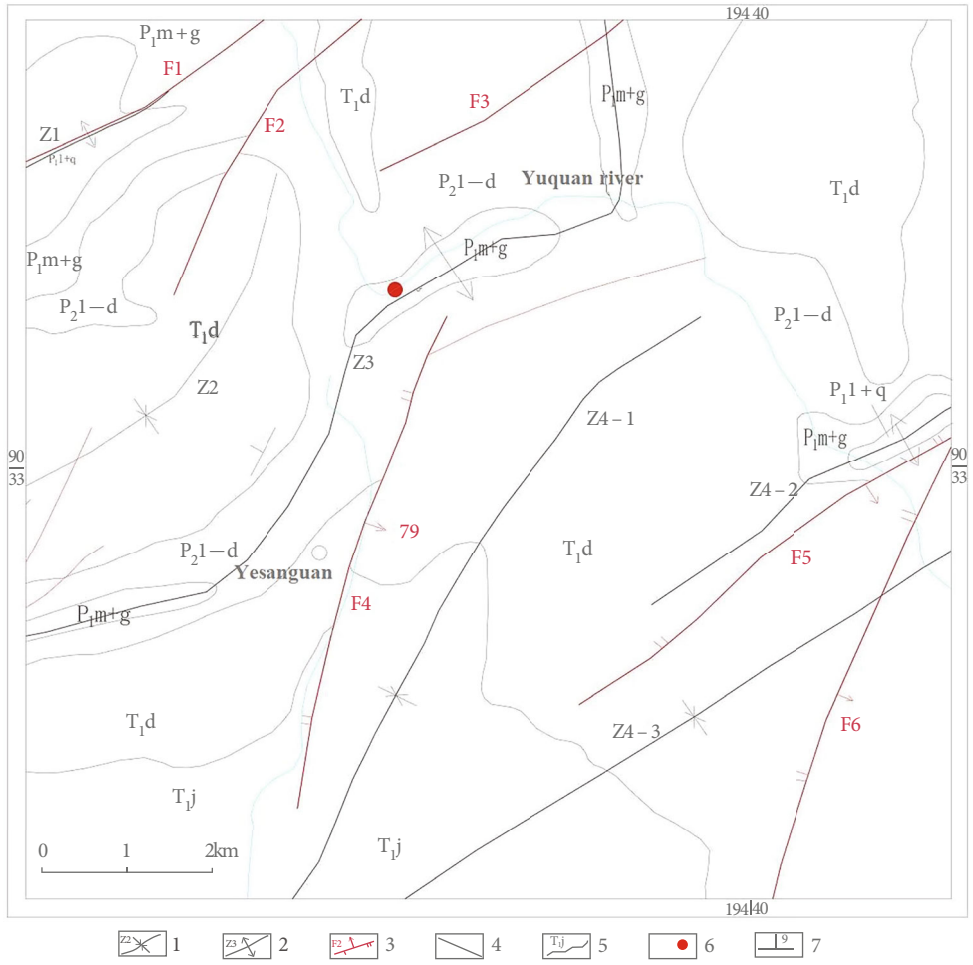

Figure 2: Outline map of geological structure of exploration area. 1, syncline and number; 2, anticline and number; 3, compressional torsional fault and its number; 4, general fault; 5, stratum code and boundary; 6, study area; 7, occurrence.

deformation mode of the Tanziyan landslide, the fracture will gradually develop to the northeast (right). The deformation zone is shown in Figure 4.

The collapse source area of the Tanziyan landslide is mainly the ghaut and the isolated peak at the top, and the depression on both sides is the potential deformation

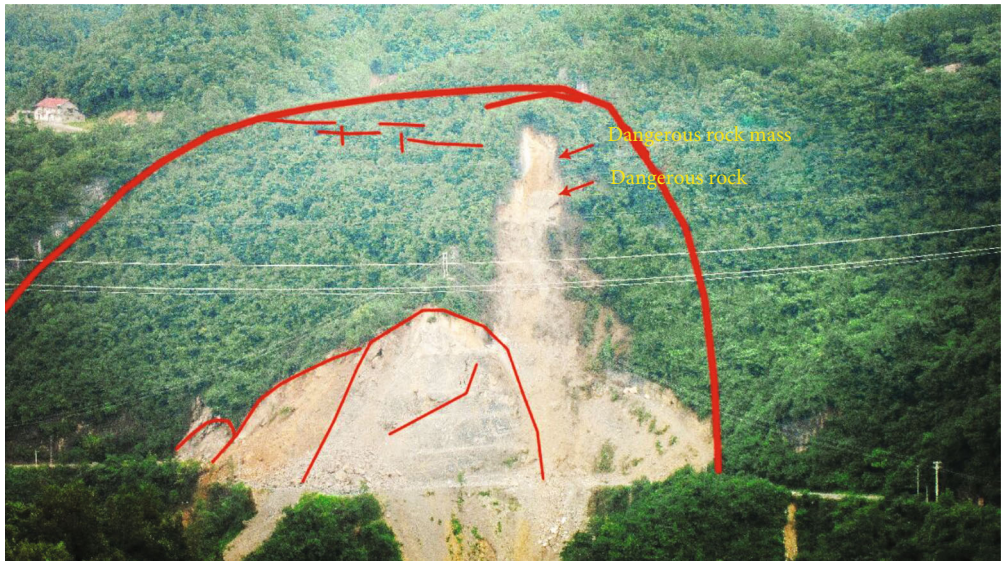

Figure 3: Overall view of Tanziyan landslide.

influence area. The collapse accumulation area is located along the national highway. Most of the deposits are distributed on the G318. A small part of the collapse block stones are scattered on the slopes and grooves above and below the national highway.

3. Deformation and Failure Mechanism

3.1. Deformation and Failure Phenomenon. The deformation of the Tanziyan landslide is mainly characterized by slides, mountain fissures, and collapse.

3.1.1. Sliding. The slide deformation occurs at the inner slope of G318 at the front edge of collapse, with a total of 3 places developed, namely, TH1, TH2, and TH3 (Figure 5), which are closely arranged from east to west. After the occurrence of slide TH1 and slide TH2, the professional monitoring of slide TH3 was focused. According to the professional deformation monitoring records, the displacement of collapse body was 0.3 m from June 30, 2018, to July 5, 2018 (Figure 6). In addition, from June 25, 2018, to June 30, 2018, the monitoring results of the high-pressure electrode slope on the upper part of the collapse TH3 were cracks, and the mountain displacement was 3.8 cm.

3.1.2. Mountain Fissures. Mountain fissure is one of the main deformations in the area, in which fissure LF2 and fissure LF3 are tension fissures and fissure LF1 is shear fissure. The fissure mentioned above LF3 with intense deformation forms a huge drawing crack trough at the ridge, showing a "thin strip of sky" landscape, which makes a vast rock mass wanting to separate from the rear mountain in the shape of a solitary peak. The three mountain fissures described in this paper are shown in Figure 7.

3.1.3. Collapse. Collapse is the primary deformation geological disaster in the area, with rich collapse source materials, poor integrity, high potential energy, and great harm. Affected by tectonism, the rock joints and fissures in this area are developed, and the cracks have apparent damage control on the rock mass. Five groups of fractures are mainly set in the study area, of which the rock stratum level and LX1 fracture (Figure 8(a)) are the principal structural planes of rock mass, with strong ductility. At the same time, it is cut by other groups of fractures, and the rock mass presents structural characteristics such as layered block fracture and rhombic wedge. As shown in Figure 8(b), LX2 and LX3 are conjugate fractures, developed in the shallow surface with good elasticity, with an extended height of 1.2-2.0 m, a length of 15 m can be seen locally, and the cutting layer is developed.

(1) Distribution of Dangerous Rock Mass. According to the field survey, after the collapse, two dangerous rock masses (W1 and W2) and one dangerous rock (W3) are mainly developed, of which dangerous rock masses W1 and W2 are distributed at the isolated peak at the trailing edge and dangerous rock mass W3 is distributed at the bottom of the cliff. According to relevant data statistics, the three dangerous rock masses all collapsed on June 25, 2018, with a total volume of about 2460 m^3, and there is a possibility of collapse again. The specific distribution is shown in Figure 9.

(2) Characteristics of Talus Slope. Most of the collapsed block stones in the area roll down to the Yuquan river valley (Figure 10(a)), with a volume of about 650m^3, a small part is accumulated at G318 (Figure 10(b)), and sporadic block stones are scattered on the groove slope. The plane of collapse accumulation body is long strip, with different thickness, thin at the top and thick at the bottom, with a thickness of 2.5-5 m. It is mainly composed of broken stones, with different diameters and angular shapes. The rock property of broken stones is flint nodule limestone.

(3) Deformation and Failure Characteristics. On June 25, 2018, Tanziyan landslide occurred and toppled northwestward. Blocked by the mountain mouth, it turned to the

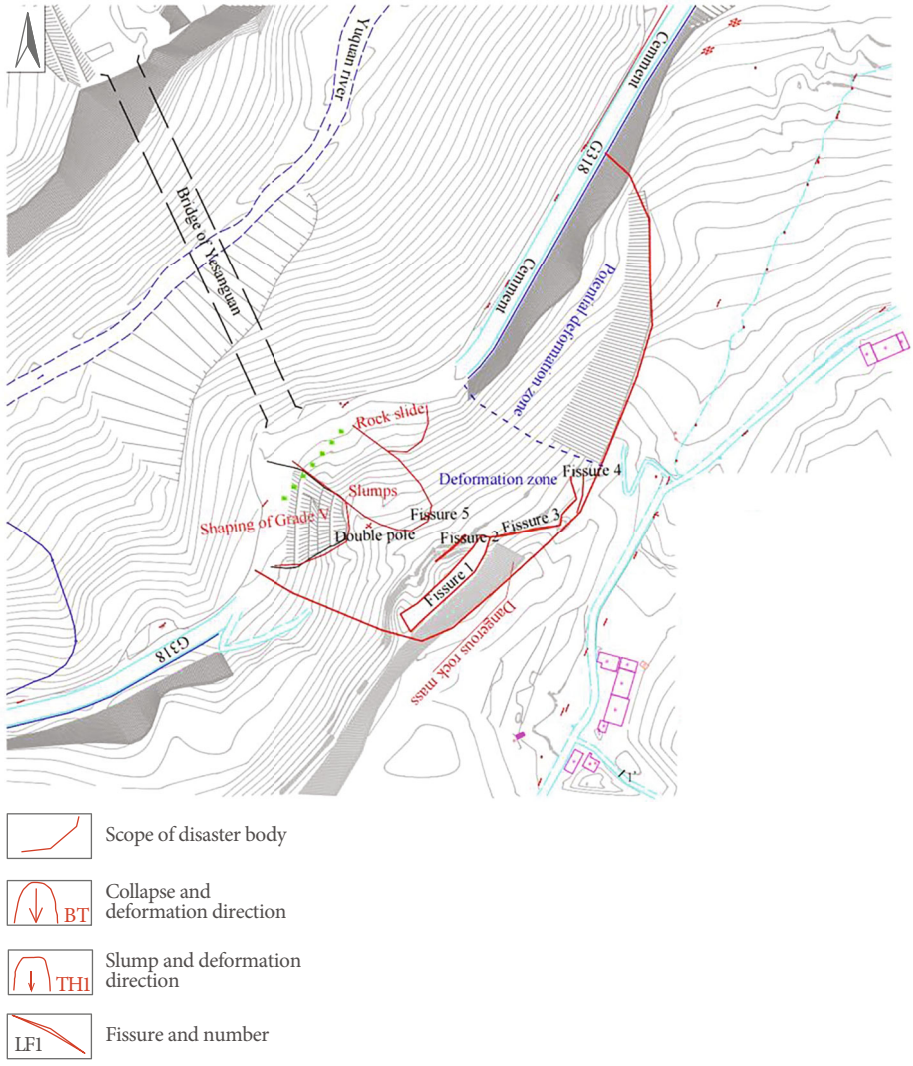

Figure 4: Plan diagram of Tanziyan landslide geological hazard.

(a) (b) (c)

Figure 5: Location distribution of slump cloth.

280° direction and rolled down with a high drop, with great potential energy and great damage. Nearly 60 m guardrails and embankments of the national highway were destroyed, and another culvert and 100 m drainage ditch were destroyed, resulting in the blockage of the national highway (Figure 10(b)).

3.2. Main Influencing Factors. According to the analysis of the characteristics of Tanziyan landslide and the main characteristics of recent deformation, the factors affecting the stability of collapse body can be divided into internal factors and external factors. The internal factors are related to the environmental geological conditions and their own characteristics of the

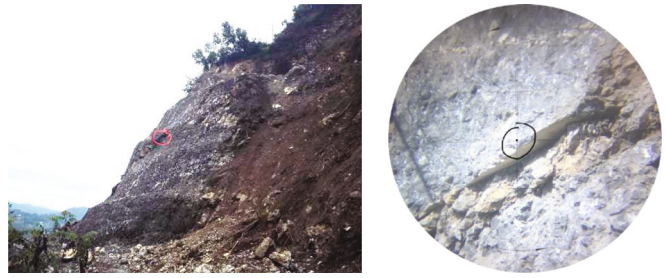

(a) (b)

Figure 6: Drawing and operation drawing of slide monitoring point.

(a) (b) (c)

Figure 7: Fissure of Tanziyan landslide geological disaster.

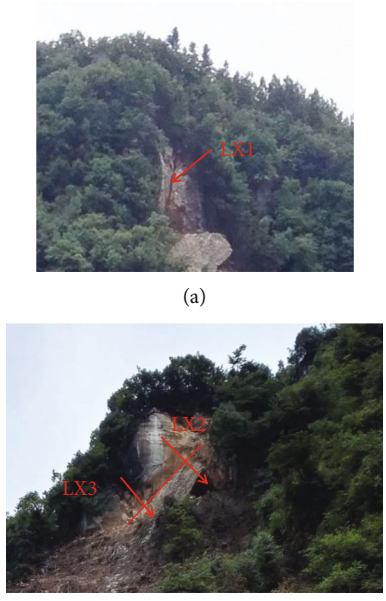

(a)

(b)

Figure 8: Distribution of joints and fissures in the investigation area.

collapse area, mainly including the geological structure, landform conditions, material structure conditions of the collapse body, and the vegetation coverage of the slope. The external factors are mainly atmospheric precipitation and human engineering activities.

3.2.1. Landform and Hydrology. The slope where the collapse area is located is steep, the height difference between the top and bottom of the collapse source is about 115.2 m, the collapse height difference is 237 m, and the slope is 37°~60°. The collapse source area has a good free surface (slope 60°). The mountain slope has good catchment conditions, and the surface water scouring is strong during rainfall. At the same time, the lush vegetation on the slope has obvious root splitting effect, which is easy to form a channel for atmospheric precipitation to infiltrate into the underground, and the underground water accelerates the weathering and dissolution of rock mass.

3.2.2. Stratigraphic and Structural Conditions. The formation lithology is mainly chert nodule limestone in Maokou Formation (P_1m) of Lower Permian system, followed by Quaternary eluvial deluvial deposit, colluvial deluvial deposit, and artificial accumulation. The rock stratum tends to northwest with an inclination of 34-37°. The slope is a clockwise slope. The material structure is as follows: the collapse area is mainly affected by structure, with broken rock mass and poor integrity. The shallow fractures of Maokou Formation (P_1m) of Lower Permian system are extremely developed, with many straight fracture surfaces and long extension, and karst fractures are also developed. The surface is covered with quaternary eluvial deluvial block stone and soil with loose structure, which is conducive to rainfall and surface water infiltration.

(a)

(b)

Figure 9: Distribution of dangerous rock masses in the survey area.

(a)

(b)

Figure 10: Distribution of colluvium block stones at river bottom (a) and G318 (b).

3.2.3. Rainfall. The infiltration of atmospheric rainfall will fill the relatively developed cracks and form hydrostatic pressure, which is very unfavorable to the stability of rock mass.

3.2.4. Human Engineering Activities. The national highway cut slope is built at the front edge to form a rock slope with a height of 10-25 m, which makes the free space conditions at the front edge well. In addition, recently human engineering activities have cleared the front edge dangerous rocks and cut the slope locally, which makes the slope stability worse.

3.3. Formation Mechanism. In the late 1970s, the slope cutting of G318 caused the rock mass at the top of the slope to crack and move down, with slight signs of deformation, but the cracks have occurred. In the long-term development process, the rainfall fills the cracks, the formed hydrostatic pressure is not conducive to the stability of the slope, the cracks continue to develop and expand, the mountains outside the cracks slowly incline outward, and the stress is concentrated at the foot of the slope. Recently, due to the slope cutting at the slope toe due to engineering construction, the state that has tended to be balanced has been broken. Recently, heavy rainfall has intensified the deformation, resulting in overall instability and collapse. The local collapse makes the whole in the limit equilibrium state again. On the whole, the slope rock mass fracture surface tracks the unloading surface and layer along the slope direction, forms a stepped fracture zone, and gradually develops into a weak surface. Once the weak surface is connected, driven by the upper rock mass, the rock mass slides along the weak surface, and a larger scale collapse will be formed.

The development process of Tanziyan collapse and slide can be roughly divided into three stages:

(1) Tensile deformation stage: when the slope toe is excavated, the massive rock mass tracks the structural cracks perpendicular to the slope direction, which produces tensile deformation. In the later stage, under the action of weathering and rainfall, the cracks gradually opens and expands, and the whole rock mass tilts outward slowly

(2) Bending deformation and failure stage: after the rock mass tilts outward, the stress concentration is formed at the weak part of the slope surface. Under the action of its own gravity, the stress gradually increases, and finally, the rock mass is unloaded and crushed in here, forming a weak broken structural plane between layers and slowly forming a sliding surface gradually penetrating from the layer surface and the unloading crack surface

(3) Cracked again to form a connected sliding surface and sliding stage: due to the recently slope cutting, the slope body temporarily in a stable state has lost its support end, and then, the upper rock mass tilts outward again and produces tensile deformation. The deep and long drawing crack trough at the rear edge is resurrected which is deepened, widened, and extended, and the upper rock mass is separated from the parent rock and has the potential of toppling and loading. Under its promotion, the early formed sliding surface tends to penetrate, and the rock mass is damaged along the sliding surface to form large-scale collapse

To sum up, the deformation and failure mode of Tanziyan landslide is fracture-bending-tensile fracture again and track the sliding failure of the weak surface. According to the deformation characteristics of the top drawing crack trough, it is wide at the top and slightly narrow at the bottom

and wide in the southwest and narrow in the northeast and gradually pinches out. It was analyzed that the rock mass outside the pull drawing crack trough is inclined outward and "tears" the mountain under the action of its own gravity. If the pull fracture continues to develop, it is bound to affect the potential deformation area and then form larger-scale deformation.

4. Stability Analysis

4.1. Calculation Method and Principle. The deformation and failure mode of Tanziyan landslide geological disaster is that the trailing edge unloading crack opens, topples outward under the influence of adverse factors such as rainfall, increases and deepens the crack opening, and finally produces overall sliding failure along the structural plane. Based on its deformation form and "Technical regulations for building slope engineering" (BG50330-2013), the stability of sliding along the structural plane is calculated. This example is more suitable for the calculation method of complex plane sliding surface, the calculation diagram is shown in Figure 11, and its calculation formula is as follows:

$$F_s = \frac{R}{T}, \tag{1}$$

$$R = [(G + G_b)\cos\theta - Q\sin\theta - V\sin\theta - U]\tan\varphi + cL, \tag{2}$$

$$T = [(G + G_b)\sin\theta + Q\cos\theta + \nu\cos\theta], \tag{3}$$

$$V = \frac{1}{2}\gamma_w h_w^2, \tag{4}$$

$$U = \frac{1}{2}\gamma_w h_w L. \tag{5}$$

In the above formulas, T is the sliding force caused by unit width strategy of sliding body and other external forces (KN/m); R is antisliding force caused by gravity per unit width of sliding body and other external forces (KN/m); C is cohesion of sliding surface (kPa); φ is internal friction angle of sliding surface (°); L is sliding surface length (m); G is dead weight per unit width of sliding body (KN/m); G_b is vertical additional load per unit width of sliding body (KN/m), taking positive value when pointing downward and negative value when pointing inward; θ is inclination angle of sliding surface (°); U is total water pressure per unit width of sliding surface (KN/m); V is total water pressure per unit width on the steep fracture surface at the trailing edge (KN/m); Q is horizontal load per unit width of sliding body (KN/m), taking a positive value when pointing to outside slope and a negative value when pointing to inside slope; h_w is the water filling height of the steep fracture at the trailing edge (m), and it is determined according to the crack conditions and catchment conditions.

4.2. Determination of Calculation Profile. Through the deformation range and stratum change delineated by the in situ ground engineering geological mapping, the deformation characteristics are analyzed structurally, and the section line is drawn in field, and the unit width is taken for research during calculation. According to the deformation, the stability is calculated as the 1-1′ longitudinal section and the G318 above section (Figure 12).

4.3. Calculation Parameters and Working Conditions

4.3.1. Calculation Parameters. The basic calculation parameters in this paper are taken according to the engineering geological survey report and the specification of "rock mechanics parameters manual" (water resources and Hydropower Press).

The natural density of rock is 2.69~2.71 g/cm^3, and the saturated density is 2.72~2.75 g/cm^3. The natural shear strength of medium thick layered limestone is as follows: C value is 1320 kPa, tgφ value is 1.43, and φ value is 55.03°. The deformation area of the project is affected by the structure, and the rock mass is relatively broken, so its strength should be much lower than that of the complete rock. According to the survey, the slope surface fractures are relatively developed and mostly open and the combination is poor. Two groups of "X" shaped main control fractures are developed in the rock mass and extend for a long time. The deformed area slides along the main control fractures. According to the geotechnical test results of the surrounding works and the reference empirical data, the complete chert nodule limestone exposed by the collapse is relatively hard rock, with saturated uniaxial compressive strength of 35 MPa and C value of more than 1000 kPa; φ value is 53°. However, the mechanical strength of the deformation and failure area is reduced due to the fracture of rock mass, which should be greatly reduced when the parameters are taken, so as to be more in line with the actual deformation situation. According to the technical code for building slope engineering, the shear strength of rock mass structural plane is taken as follows:

(1) Considering the importance of the slope, the standard value of shear strength is the corresponding value of "general combination": C value is 90 kPa and φ value is 35°

(2) The value of natural shear strength of potential slip surface is as follows: C value is 90 kPa and φ value is 35°; the saturated shear strength is multiplied by the reduction factor of 0.9, and the C value is 80 kPa and φ value is 32°

According to relevant data, the basic seismic intensity of Badong County is grade VI, and the peak ground acceleration is 0.05 g.

4.3.2. Calculation Conditions. According to the hydrogeological conditions, there is almost no water in the rock mass at ordinary times. The combination of calculation conditions is as follows: working condition 1: dead weight; working condition 2: dead weight+20-year rainstorm; and working condition 3: dead weight+earthquake (VI degree fortification).

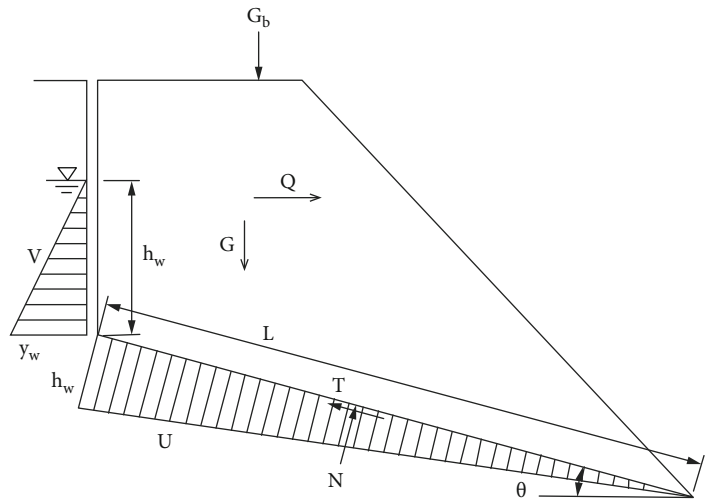

Figure 11: Structural plane stability calculation diagram.

4.4. Calculation Results and Analysis. According to the calculation model and parameters, the stability coefficient of disaster body under different working conditions is calculated. The calculation results are shown in Table 1. The evaluation shall refer to the provisions in relevant specifications.

The calculation results show that the stability coefficient of Tanziyan is 1.065 under condition 1, which is basically stable, and the safety margin is not high, indicating that Tanziyan is basically stable due to unloading under natural condition. It is in an unstable state under condition 2. Rainfall will fill the cracks on the top of the slope and form hydrostatic pressure, and the stability coefficient drops sharply, so that the slope is in an unstable state. Under condition 3, the stability coefficient is 1.038, which is understable. Considering various working conditions, the disaster body is from understable to unstable state, and engineering treatment is urgently needed to improve the stability coefficient.

5. Treatment Measures

According to the deformation characteristics and causes of Tanziyan landslide, slope cutting and shaping is adopted to eliminate dangerous rocks and improve the overall stability. For multiple cracks developed at the top, the form of crack sealing is adopted to prevent rainfall infiltration along the cracks. In order to further improve the overall stability, the construction method of lattice structure combined with anchor cable is adopted for anchoring.

5.1. Slope Cutting and Shaping

5.1.1. Conceptual Design. According to the height difference and slope of the landslide mass, the 1-1′, 2-2′, and 3-3′ sections in the deformation area are cut at a slope ratio of 1 : 1, as shown in Figure 13. And cut the slope at the slope ratio of 1 : 0.75 for sections 4-4′ and 5-5′, as shown in Figure 14. Each grade of slope is 15 m high and the middle berm is 2 m wide. The slope cutting and shaping area is 16210 m^2, and the slope cutting volume is about 104676 m^3.

The berm can be reasonably set according to the original landform of the northeast slope (potential deformation area). The north-east side of the slope cutting area shall be smoothly connected with the original landform, and the slope ratio shall be controlled at 1 : 2. If the smooth connection cannot be made due to the thick soil layer, the slope can be made according to the slope ratio of 1 : 1, and then, lattice anchor bolt shall be used for support. Although no one lives below the construction area, the bottom of the slope is the Yuquan river, and the waste slag cannot be rolled down arbitrarily to avoid blocking the river and forming a barrier lake. Before slope cutting, sand bags shall be stacked outside the national highway for buffer, with a length of 190 m, a height of 2 m, and a bottom width of 3 m. The waste slag shall be removed in time to ensure that the top is stable and cannot be carried out at the same time as slope cutting.

5.1.2. Stability Review. The slope cutting and shaping project basically eliminates the sliding deformation and failure controlled by the structural plane, but the downward extension distance of the crack is not clear in the top tensile crack groove. The rock mass after slope cutting forms a wedge under the joint action of the layer and the downward extension crack of the tensile crack groove, which may deform along the layer. Therefore, the bedding stability shall be rechecked according to the slope shape after slope cutting and shaping. The parameters are the same as above, and the calculation model is shown in Figure 15.

Through calculation, under condition 2, the stability factor is 1.017, which is in an unstable state and has not yet reached the safety factor of 1.1 required by the design. For the slope after shaping, other projects still need to be used for further support.

Through calculation, under condition 2, the stability factor is 1.017, which is in an unstable state and has not yet reached the safety factor of 1.1 required by the design. For the slope after shaping, other projects still need to be used for further support.

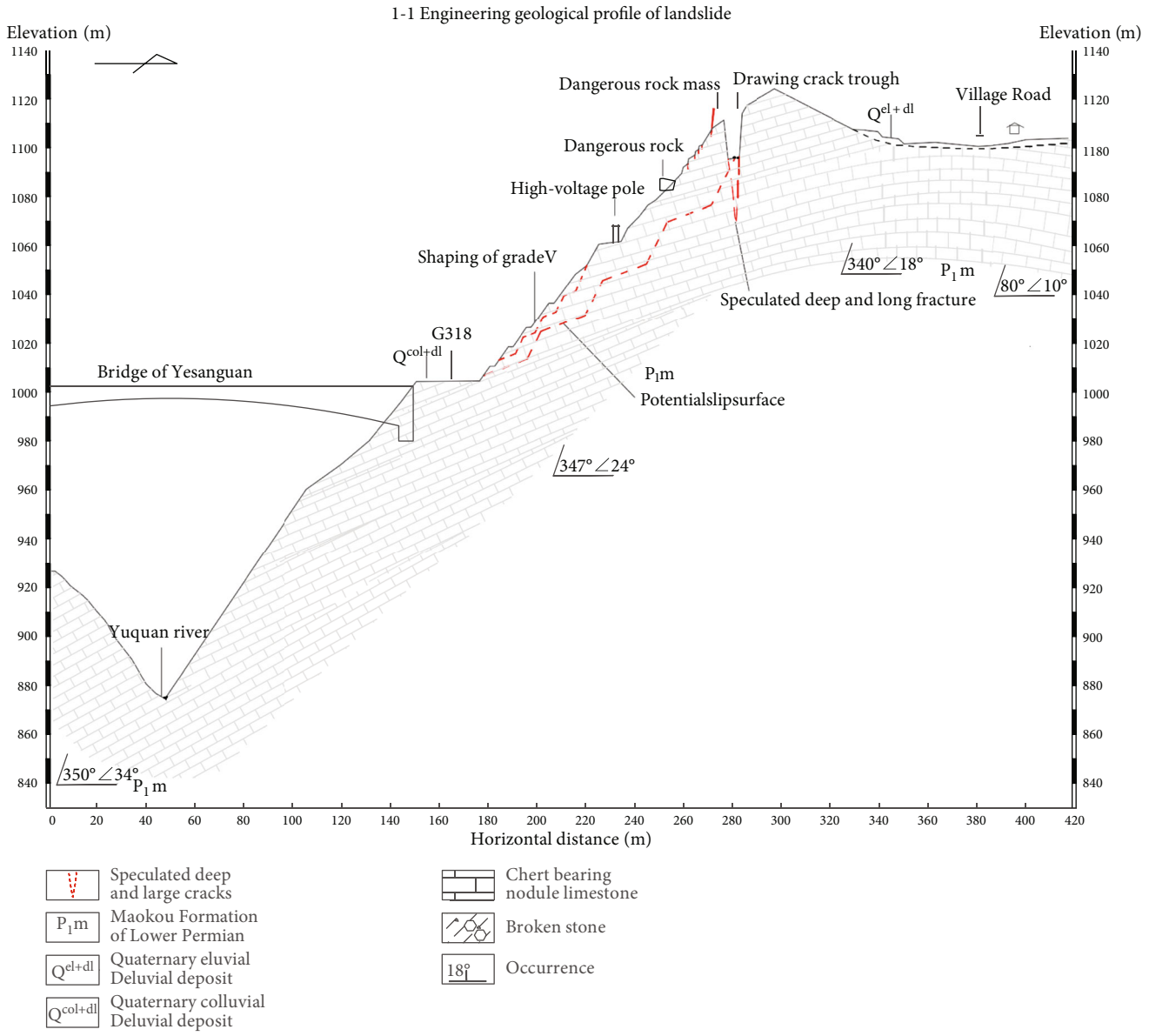

Figure 12: Calculation diagram of profile above G318.

Table 1: Stability calculation results of Tanziyan landslide geological hazard.

Profile number	Calculation condition	Stability factor Fs	Evaluate
1-1′	1	1.065	Basically stable
	2	0.895	Unstable
	3	1.038	Understable

Attention: stable, $Fs \geq 1.15$; basically stable, $1.05 \leq Fs < 1.15$; understable, $1.0 \leq Fs < 1.05$; unstable, $Fs < 1.0$.

5.1.3. Drawing Crack Trough Slope Cutting. The slope surface improves its own stability through slope cutting, but the rear edge wall of the cleavage groove after slope cutting forms a steep cliff with a height of nearly 20 m. Although the investigation shows that its stability is good at this stage and the crack cutting is not obvious, under the influence of long-term weathering, rainfall, and other adverse factors, it is inevitable that there will be block falling. If it is not treated, it will still become a hidden danger in the future. In combination with the landform developed by the tensile groove and the local construction planning for the area, it is proposed to eliminate the hidden danger by cutting the slope on the top of the mountain.

5.2. Crack Sealing. At present, many cracks are developed at the top of the slope. The maximum extension length of these cracks can reach more than 20 m and the opening width can reach 0.5 m. The development of cracks is very conducive to the infiltration of surface water formed by rainfall and is very unfavorable to the stability of the slope.

The method of clay compaction and concrete sealing is adopted in this paper. The slope excavation shall be carried

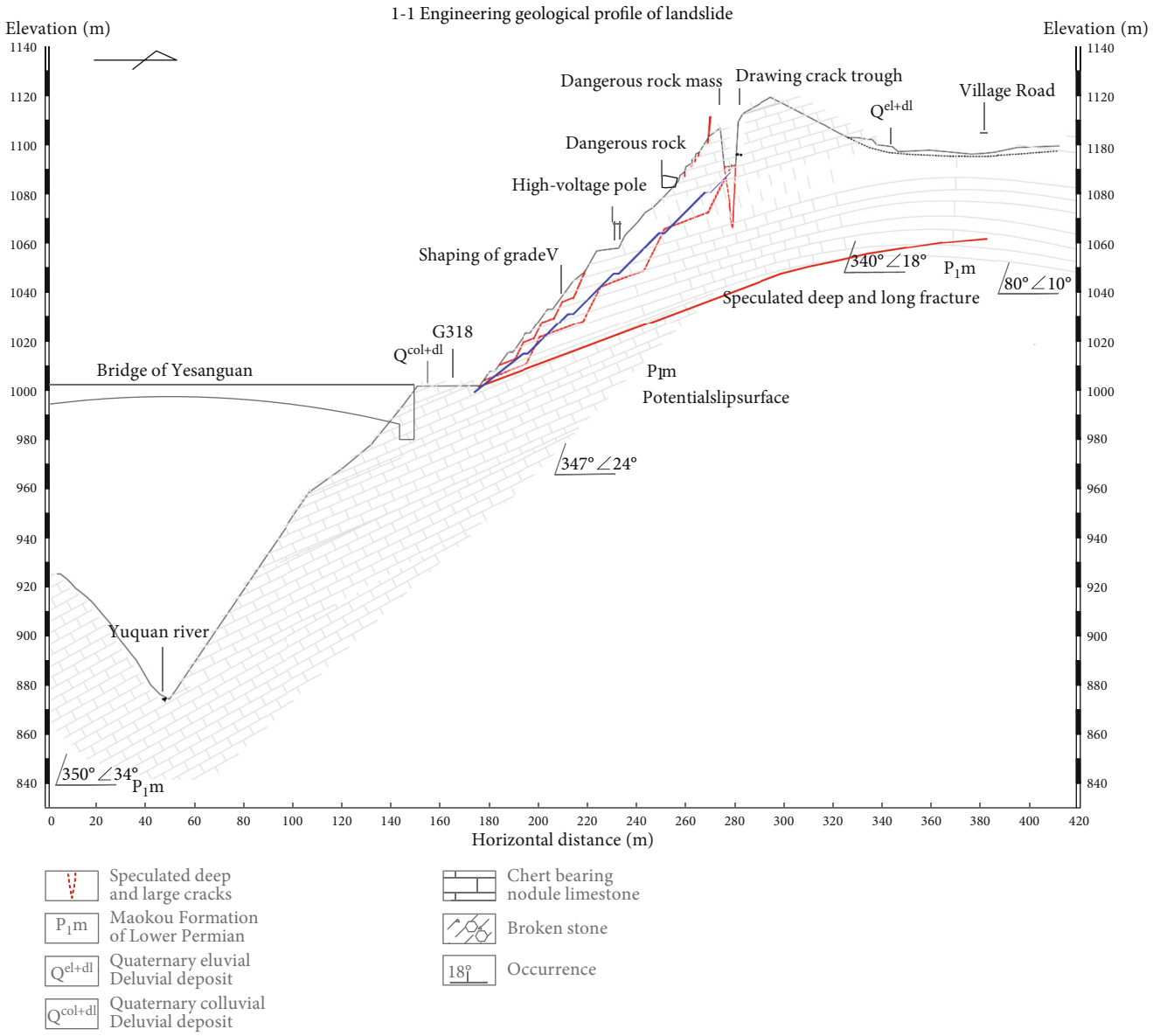

Figure 13: Schematic diagram of 1-1′ section slope cutting.

out on both sides of the existing crack according to 1 : 0.75, and the excavation depth shall not be less than 1 m, and then, the clay shall be backfilled and compacted by machinery. The top of the crack is sealed with concrete. The concrete slab is 0.3 m thick. It is cast in situ with C20 concrete. A steel nail is embedded on both sides of the concrete every 5 m. After the concrete curing, the steel nail is numbered for simple crack monitoring.

5.3. Lattice. The slope after slope cutting and shaping is further anchored with lattice anchor cable. The lattice is arranged at an elevation of 1000~1095 m, and edge sealing beams are used around and inside and outside the berm. The total area of the lattice structure is 16210 m^2, and the anchor cable is arranged at the intersection of the lattice structure, with the length of 20~55 m.

The slope protection adopts reinforced concrete lattice structure, the frame is arranged in a square shape, the side length is 4 m × 4 m, and the beam section is 50 cm × 65 cm (width × high). The bottom of the lattice structure is directly connected to the concrete retaining wall. A total of 12 rows of anchor cables are arranged at the intersection of the lattice structure of an elevation of 1920-1980 m, and grass is planted with the frame.

5.4. Anchor Cable and Rock Bolt. A total of 12 rows of anchor cables are arranged in the middle of the slope cutting and shaping area. The length of anchor cables is based on passing through the potential sliding surface and tensile crack groove. Eight kinds of anchor cable lengths are determined through calculation. Through engineering analogy and referring to relevant regulations, the length of anchor

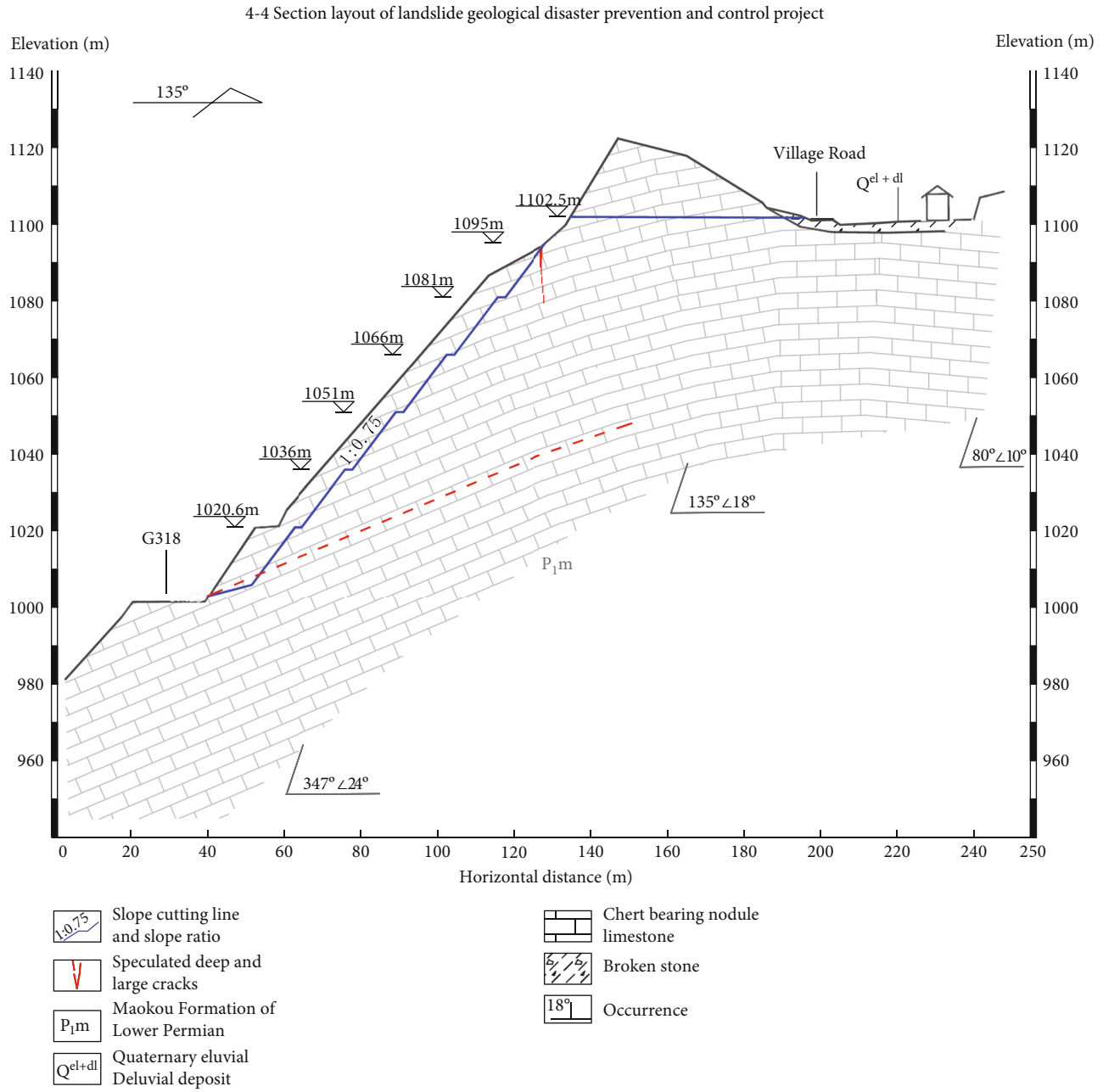

Figure 14: Schematic diagram of 4-4′ section slope cutting.

sections is 5 m. The nonfully bonded prestressed anchor cable is selected. The horizontal and vertical spacing of the anchor cable is 4 m. The shooting direction of the anchor cable is roughly perpendicular to the dip direction of the rock stratum, and the included angle between the incident angle and the horizontal angle is 25°. The anchor cable is arranged at the intersection of the lattice beam. The anchor pier is directly built on the lattice beam with concrete to form a table perpendicular to the incidence of the anchor cable. After the pretensioning of the anchor cable, the anchor head is poured with concrete.

Rock bolts are arranged at the intersection of anchor cables at the end of lattice beam. The rock bolts are made of C25 reinforcement. The rock bolts are 6 m and 9 m long, arranged alternately in quincunx shape, and the included angle between the incident angle of rock bolts and the horizontal angle is 25°. The rock bolts is of full bonding type and does not need to be pulled out.

5.5. Retaining Wall. There are 2 retaining walls, which are, respectively, arranged on the inside and outside of the highway. The retaining wall inside the highway can support the lattice beam and improve the overall aesthetics. The back side of the retaining wall in the nonlattice slope protection area does not need to be backfilled, and at least 2 m is reserved from the slope toe to form a rockfall groove. The retaining wall outside the highway is used to repair the damaged shoulder, and it shall be repaired according to the damage. The wall body is poured

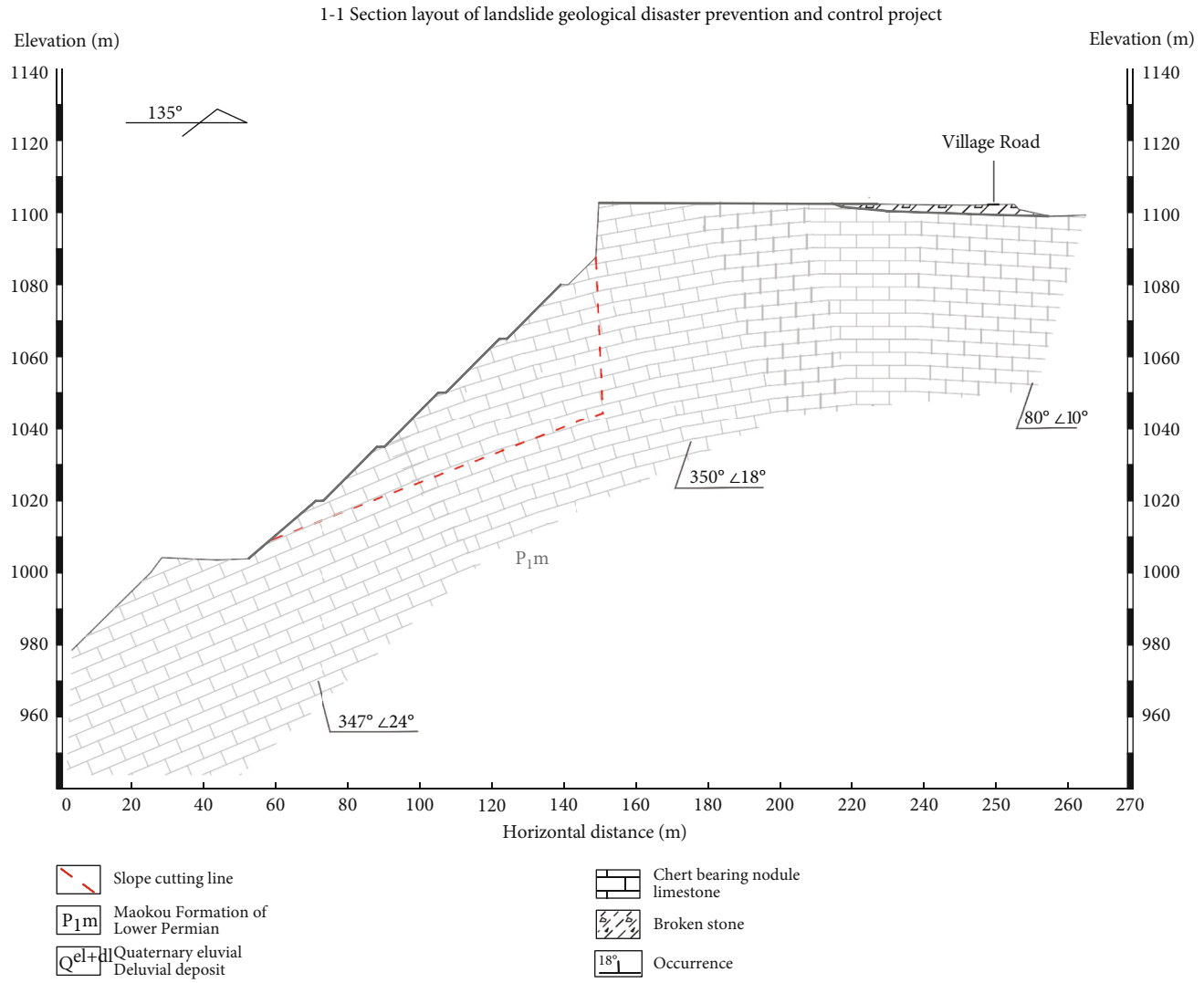

Figure 15: Stability calculation profile of 1-1′ section after slope cutting and shaping.

Table 2: Calculation results of retaining wall.

Retaining wall number	Antisliding K_c	Resistance to capsizing K_o	Foundation stress and eccentricity				Wall bottom section strength		
			e	σ_1 (kPa)	σ_2 (kPa)	σ (kPa)	$e1$	σ (kPa)	τ (kPa)
D01	2.076	4.013	0.129	96.537	42.648	69.592	0.129	96.537	-7.721
Repair the road shoulder	2.553	3.050	0.143	115.242	21.382	68.312	0.143	115.242	-11.269
Results evaluation	>1.3	>1.5	Comply with relevant specifications						

with C25 concrete, and expansion joints are set every 15 m. The foundation of the retaining wall and behind the wall is medium thick layered chert nodular limestone. There is no need to slope during foundation excavation. A drainage hole is set on the wall body, and the upstream side is wrapped with geotextile.

After checking and calculating a series of soil mechanics formulas, the antisliding stability, antioverturning stability, foundation bearing capacity, wall bottom section strength, and impact resistance of masonry retaining wall meet the planning requirements. The calculation results are shown in Table 2.

5.6. Slope Surface Greening. Vegetation restoration is carried out on the slope based on the principles of green treatment and ecological treatment. For slope greening, ecological bags are mainly placed in the lattice frame, and grass seeds are mixed in the soil, which is conducive to plant growth. With polypropylene as the main raw material, the ecological bag has the functions of antiultraviolet, antiacid, alkali and salt, antimicrobial erosion, and water and soil permeability, and the molding specification is 880 × 300 × 200 (mm). The ecological bag is laid horizontally on the long side. After laying, the surface of the ecological

bag has a space of 10 cm from the top of the lattice beam to avoid unstable factors caused by the prominent lattice of the ecological bag.

5.7. Active Protective Net. After slope cutting and shaping, a 20 m high cliff is formed on the east side wall (parent rock) of the original tensile fracture groove. Although the whole is relatively complete and the fracture cutting degree is slight, under the action of long-term weathering, rainfall, and other adverse factors, blocks may fall off and pose a threat to the vehicles below. In order to prevent the slope from forming new dangerous rock disasters again after risk removal, STG-50 active protection system is designed to protect the rock wall.

The active flexible protective net covers the whole exposed slope, from the upper part to the cliff top and from the lower part to the lattice top beam in the slope cutting area. The slope area to be protected is 600 m^2, and 870 m^2 active protective net is laid.

6. Conclusions

Through geological investigation, this paper studied the stability, deformation, and failure characteristics of the disaster body in this area, puts forward corresponding treatment measures, and draws the following conclusions:

(1) The whole is from understable to unstable state

(2) The development process of Tanziyan landslide can be roughly divided into three stages, namely, tension fracture deformation stage, bending deformation failure stage, and retension fracture and forming a through sliding surface instability and sliding stage

(3) In view of the landslide situation in this paper, it is proposed to adopt slope cutting and shaping, crack sealing and filling, lattice structure, anchor cable, retaining wall, slope greening and active protection network, and combined with the monitoring scheme

With the current research, the research on landslide stability analysis method and deformation failure mode is relatively mature, and the materials and schemes for landslide control emerge endlessly. The complex plane sliding surface calculation method used in this paper is only one attempt. Some methods, theories, and treatment measures mentioned in Introduction, such as the application research of negative Poisson's ratio anchor cable, need more engineers and technicians to verify and develop.

Data Availability

The data that support the conclusions of this study are available from text and the corresponding author upon reasonable request.

Conflicts of Interest

There are no conflicts of interest with respect to the results of this paper.

Acknowledgments

This study is sponsored by the National Natural Science Foundation of China (No. 42162026).

References

[1] Y.-F. Yao, "Study on failure mode and development mechanism of anti-dip rock landslide," *Chemical Minerals and Processing*, vol. 50, no. 7, pp. 49–52, 2021.

[2] B.-F. Liu, X. Liang, and K. Zhou, "Study on the genetic mechanism and treatment scheme of a landslide," *Subgrade Engineering*, vol. 2, pp. 231–236, 2021.

[3] H.-T. Zhang, D.-C. Zhu, and P. Wang, "Analysis of deformation and failure mechanism of bedding rock slope," *Highway*, vol. 66, no. 3, pp. 67–71, 2021.

[4] Q.-L. Zeng, W.-F. Wang, and H.-Y. Chen, "Study on characteristics of Zhaojiagou landslide in Zhenxiong and instability mechanism based on slope structure," *Journal of Engineering Geology*, vol. 24, no. 4, pp. 510–518, 2016.

[5] Y. Zhang, S.-R. Su, and P. Li, "Study on landslide mechanism of fault control – taking Liujiapo landslide as an example," *Journal of Engineering Geology*, vol. 23, no. 6, pp. 1127–1137, 2015.

[6] Q. Xu, "Deformation and failure behavior and internal mechanism of landslide," *Journal of Engineering Geology*, vol. 20, no. 2, pp. 145–151, 2012.

[7] X.-L. Hu, H.-M. Tang, and C.-D. Li, "Study on deformation and failure mechanism of Baozha landslide based on parameter inversion," *Journal of Engineering Geology*, vol. 19, no. 6, pp. 795–801, 2011.

[8] X.-S. Li, K. Peng, J. Peng, and D. Hou, "Experimental investigation of cyclic wetting-drying effect on mechanical behavior of a medium-grained sandstone," *Engineering Geology*, vol. 293, article 106335, 2021.

[9] X.-S. Li, K. Peng, J. Peng, and H. Xu, "Effect of cyclic wetting-drying treatment on strength and failure behavior of two quartz-rich sandstones under direct shear," *Rock Mechanics and Rock Engineering*, vol. 54, no. 11, pp. 5953–5960, 2021.

[10] Y. Wang, B. Zhang, B. Li, and C.-H. Li, "A strain-based fatigue damage model for naturally fractured marble subjected to freeze-thaw and uniaxial cyclic loads," *International Journal of Damage Mechanics*, vol. 30, no. 10, pp. 1594–1616, 2021.

[11] M.-Z. Gao, J. Xie, Y.-N. Gao et al., "Mechanical behavior of coal under different mining rates: a case study from laboratory experiments to field testing," *International Journal of Mining Science and Technology*, vol. 2021, no. 31, pp. 825–841, 2021.

[12] M.-Z. Gao, J. Xie, J. Guo, Y.-Q. Lu, Z.-Q. He, and C. Li, "Fractal evolution and connectivity characteristics of mining-induced crack networks in coal masses at different depths," *Geomechanics and Geophysics for Geo-Energy and Geo-Resources*, vol. 7, no. 1, 2021.

[13] C. Zhu, Y. Lin, and G. Feng, "Influence of temperature on quantification of mesocracks: implications for physical properties of fine-grained granite," *Lithosphere*, vol. 2021, no. - Special 4, 2021.

[14] D.-H. Chen, H.-E. Chen, W. Zhang, J.-Q. Lou, and B. Shan, "An analytical solution of equivalent elastic modulus considering confining stress and its variables sensitivity analysis for fractured rock masses," *Journal of Rock Mechanics and Geotechnical Engineering*, 2021.

[15] C. Zhu, M.-C. He, B. Jiang, X.-Z. Qin, Q. Yin, and Y. Zhou, "Numerical investigation on the fatigue failure characteristics of water-bearing sandstone under cyclic loading," *Journal of Mountain Science*, vol. 18, no. 12, pp. 3348–3365, 2021.

[16] G.-X. Wang, "Current situation of landslide prevention engineering measures at home and abroad," *Chinese Journal of Geological Hazards and Prevention*, vol. 1, pp. 2–10, 1998.

[17] S.-D. Yin, X.-T. Feng, and Y.-L. Zhang, "Study on parallel evolutionary neural network method for optimization of landslide reinforcement scheme," *Journal of Rock Mechanics and Engineering*, vol. 16, pp. 2698–2702, 2004.

[18] G.-X. Wang, "Key technologies and treatment methods in landslide prevention and control," *Journal of Rock Mechanics and Engineering*, vol. 21, pp. 20–29, 2005.

[19] L.-Q. Wu, F. Zhang, and X.-C. Ling, "Stability analysis of high slope in Pingtou village, Wuyi, Zhejiang Province under heavy rainfall," *Journal of Rock Mechanics and Engineering*, vol. 28, no. 6, pp. 1193–1199, 2009.

[20] L. Ma, "Study on causes and treatment measures of landslide in waste dump in open pit mine," *Coal Technology*, vol. 35, no. 8, pp. 166–168, 2016.

[21] G.-X. Wang, "Selection and optimization of landslide control scheme," *Journal of rock Mechanics and Engineering*, vol. S2, pp. 3867–3873, 2006.

[22] C. Zhu, M.-C. He, X.-H. Zhang, Z.-G. Tao, Q. Yin, and L.-F. Li, "Nonlinear mechanical model of constant resistance and large deformation bolt and influence parameters analysis of constant resistance behavior," *Rock and Soil Mechanics*, vol. 42, no. 7, pp. 1911–1924, 2021.

[23] X.-W. Zou, "Stability analysis and treatment measures of high and steep slopes of Mombasa highway," *Engineering Construction*, vol. 53, no. 8, pp. 20–25, 2021.

[24] J.-Q. Huang, "Cause analysis and treatment measures of expressway slope landslide," *Engineering Construction and Design*, vol. 13, pp. 91–93, 2021.

[25] J.-H. Cao, "Stability analysis and treatment measures of ancient landslide of Xiluodu Hydropower Station," *Water Conservancy and Hydropower Technology*, vol. 47, no. 12, 2016.

[26] Z.-G. Tao, C. Zhu, M.-C. He, and M. Karakus, "A physical modeling-based study on the control mechanisms of negative Poisson's ratio anchor cable on the stratified toppling deformation of anti-inclined slopes," *International Journal of Rock Mechanics and Mining Sciences*, vol. 138, article 104632, 2021.

[27] G. Li, Y. Hu, S. M. Tian, M. weibin, H. L. Huang, and S.-M. Tian, "Analysis of deformation control mechanism of prestressed anchor on jointed soft rock in large cross-section tunnel," *Bulletin of Engineering Geology and the Environment*, vol. 80, no. 12, pp. 9089–9103, 2021.